Polarization Effect Induced by Discrete Impurity at Semiconductor/Oxide Interface in Si-FinFET

Katsuhisa Yoshida
Institute of Applied Physics,
University of Tsukuba
Ibaraki 305-8573, Japan
yoshida@bk.tsukuba.ac.jp

Kohei Tsukahara
Institute of Applied Physics,
University of Tsukuba
Ibaraki 305-8573, Japan
s1920328@s.tsukuba.ac.jp

Nobuyuki Sano
Institute of Applied Physics,
University of Tsukuba
Ibaraki 305-8573, Japan
sano.nobuyuki.gw@u.tsukuba.ac.jp

***Abstract*—The random dopant fluctuation (RDF) is a dominant source of statistical variability for nano-scale metal-oxide-semiconductor-field-effect-transistors (MOSFETs). We study RDF with the polarization effect induced by the discreteness of impurity and the dielectric mismatch at the Si/oxide interface by 3D drift-diffusion simulation. The charge distribution model employed in this study for the discrete impurity clarifies RDF dependence on the dielectric constant of oxide material. It is shown that explicit modeling of the polarization charge associated with discrete impurities is inevitable for reliable prediction of threshold voltage.**

Keywords—discrete impurity, random dopant fluctuation, drift-diffusion method, FinFET, MOSFET, polarization

I. Introduction

The scaling of Si metal-oxide-field-effect-transistor (MOSFET) has been attained by adopting the multi-gate structure, such as FinFET [1], and high-κ oxide materials. However, nano-scaled devices are seriously suffered by statistical variability problems due to its small volume of semiconductor materials and an increase of the surface/volume ratio. The random dopant fluctuation (RDF) [2-8] is one of the crucial sources of the variability problems and unavoidable in any nano-scale devices employing a doping technique.

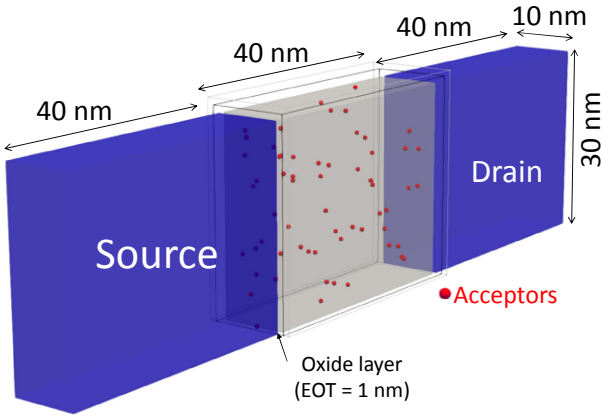

Fig. 1. Schematic of Si-FinFET structure employed in this study. In the channel region, 60 discrete acceptors (presented as red points) are randomly distributed. Source and drain regions are uniformly doped by donor concentration of 10^{20} cm^{-3} (blue shaded regions).

The physical origin of RDF is the potential fluctuation induced by the variabilities of the position and the number of dopants. In order to carry out predictive device simulation for RDF, it is inevitable to treat the Coulomb potential in the framework of the simulation [9]. In the device simulation, the Coulomb potential of discrete impurities is divided into the short-range and the long-range potentials, and those components are separately considered in the transport equation and the Poisson equation, respectively. It should be noted that the jelly dopant model corresponds to the long-wavelength limit of the long-range potential and, thus, there is no potential fluctuation.

For a bulk semiconductor, the short-range element is modeled as a screened potential by carriers in the substrate assuming charge neutral and thermal equilibrium. On the other hand, the long-range potential is the compensated part of the full Coulomb potential by carriers when we evaluate the short-range one. Therefore, once we know the distribution of screening carriers, we can regard it as a charge distribution model of the discrete impurity and obtain only the long-range potential as a solution of the Poisson equation without double-counting the short-range one. Additionally, in the nano-scale multi-gate devices, we should take care of a fact that the discreteness of impurities induces a polarization charge on the semiconductor/oxide interface due to a difference of dielectric constants.

Recently, we have reported a charge model for discrete impurities taken into account the polarization charge [10]. Since the polarization charge modifies the Coulomb potential compared to that without the interface and, thus, the charge distribution model for the long-range potential should be corrected. In this study, we carried out the drift-diffusion (DD) simulation incorporating the polarization effect at the interface associated with discrete impurities for the long-range Coulomb potential under a nano-scale FinFET operation.

II. Numerical Method

We employ a Si-FinFET device structure as shown in Fig. 1 and carry out 3D-DD simulation. The Fin structure has 10 nm of the width and 30 nm of the height. The channel length is 40 nm. The source and drain regions are uniformly doped by donor concentration of 10^{20} cm^{-3}. In the channel region, 60 acceptors are randomly distributed, and 500 different acceptor configurations are considered. Therefore, we only introduce position variation of acceptors within the channel region as a

978-1-7281-0940-4/19/$31.00 ©2019 IEEE

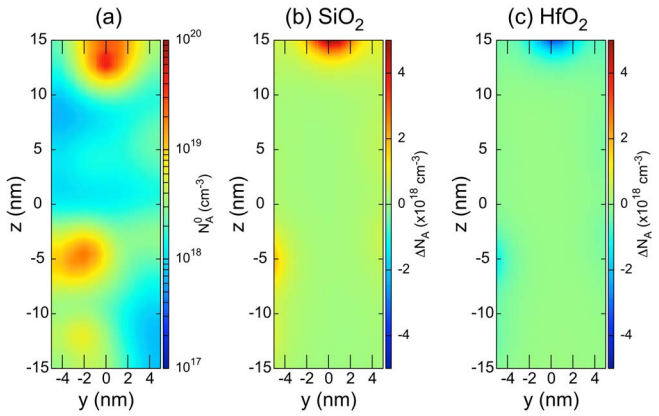

Fig. 2. Profiles of acceptor concentration in the middle corss-section of the channel region presented in Fig. 1 with the same acceptor configuration. (a) N_A^0 is acceptor concentration based on the Yukawa-like charge model for discrete impurities without polarization correction term induced by the interface. Polarization correction terms for acceptor concentration, ΔN_A, with (b) SiO_2 and (c) HfO_2 oxide layers. The acceptor concentration, N_A, used in the Poisson equation is a sum of N_A^0 and ΔN_A.

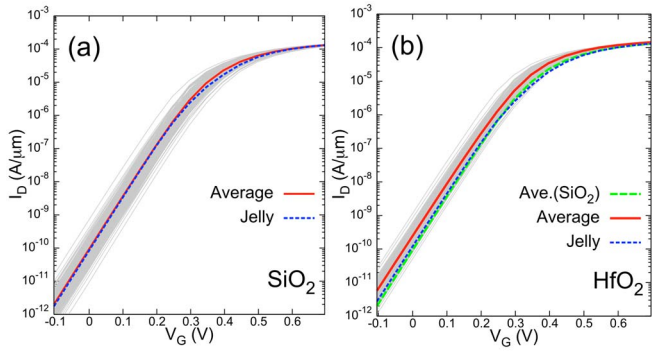

Fig. 3. I_D-V_G characteristics with 500 different acceptor configurations (gray lines) under V_D = 0.05 V. (a) SiO_2 and (b) HfO_2 oxide layers. Red solid lines are averaged value over 500 different configuration for each oxide material. The results with jelly model for each oxide material are plotted in blue dotted lines. The acceptor concentration employed in the jelly models is 5×10^{18} cm^{-3}. The green dashed line presented in (b) is the same curve named as "Average" in (a).

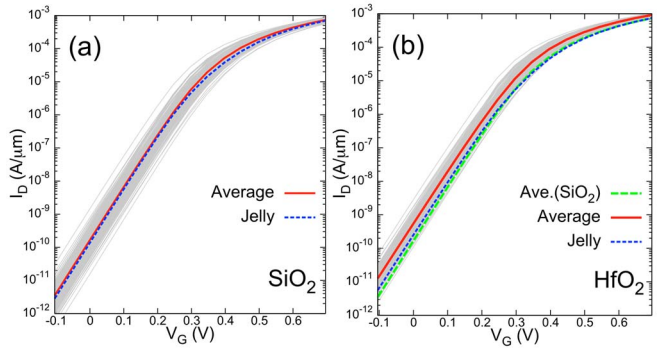

Fig. 4. I_D-V_G characteristics with 500 different acceptor configurations (gray lines) under V_D = 0.8 V. (a) SiO_2 and (b) HfO_2 oxide layers. Calculation conditions and lines are same employed in Fig. 3 except the drain voltage.

source of statistical variability in the present study. The charge distribution model for the discrete impurity and its long-range Coulomb potential is based on our recent work [10]. The acceptor concentration, N_A, used in the Poisson equation is described as,

$$N_A = \sum_i^{60}(N_{A,i}^0 + \Delta N_{A,i}), \quad (1)$$

where $N_{A,i}^0$ is the Yukawa-like acceptor distribution for the i-th acceptor and given by

$$N_{A,i}^0(\mathbf{r}, \mathbf{r}_i) = q_C^2 \exp(-q_C^2|\mathbf{r} - \mathbf{r}_i|)/(4\pi|\mathbf{r} - \mathbf{r}_i|), \quad (2)$$

where q_C is an inverse of the screening length, and $\mathbf{r}_i$ is a center of the i-th acceptor. The screening length is estimated by the Debye-Hückel or the Thomas-Fermi model depending on the concentration. $\Delta N_{A,i}$ is the polarization correction term and is functions of the difference of dielectric constants between Si and the oxide material and of the distance between the center of impurity and the interface. For convenience, we define two quantities as $N_A^0 = \sum_i^{60} N_{A,i}^0$ and $\Delta N_A = \sum_i^{60} \Delta N_{A,i}$. SiO_2 and HfO_2 are employed as oxide materials, and their thicknesses are 1.0 nm and 6.13 nm, respectively. The HfO_2 thickness is equivalent to 1.0 nm of the effective oxide thickness (EOT). The relative dielectric constants of Si, SiO_2, and HfO_2 are 11.8, 3.9, and 23.9, respectively. The acceptor concentration averaged in the channel volume is 5.0×10^{18} cm^{-3}, and the screening length is 1.63 nm at 300K. In the jelly model, the acceptor concentration in the channel region is 5.0×10^{18} cm^{-3}. The threshold voltage, V_{Th}, is defined when the drain current, I_D, exceeds 14.9 nA/μm.

III. Discussion

Fig. 2 (a) shows the acceptor concentration profile, N_A^0, without the polarization correction term in a cross-section at a middle plane of the channel region. Since we employ the Yukawa-like charge model for each acceptor, N_A^0 is widely distributed in the substrate, and its high concentration area - namely $N_A^0 > 2\times10^{19}$ cm^{-3} roughly spreads over a square of the screening length. This fact means that the charge of the discrete impurity is not a point-like charge but has a fine size to exclude the short-range potential.

Figs. 2 (b) and (c) are the distributions of the polarization correction term, ΔN_A, for SiO_2 and HfO_2, respectively, with the same acceptor configuration. The correction term ΔN_A is only distributed near the interface and rapidly decreases with distance from the oxide layer. Additionally, it indicates that a larger dielectric constant of the oxide layer than Si screens the Coulomb potential of a discrete impurity and, thus, reduces the screening carriers required to satisfy the charge neutral condition as pointed above. As a result, the correction term becomes negative to decrease acceptor concentration for the long-range potential. When the dielectric constant is smaller than Si, the opposite effect has to be taken into account and, thus, the result with SiO_2 has a positive correction value.

Figs. 3 and 4 show I_D-V_G characteristics associated with 500 different acceptor configurations under the drain voltages, V_D, of 0.05 V and 0.8 V, respectively. The results with the jelly acceptor model are also presented for each oxide material. The acceptor concentration of the jelly model is 5×10^{18} cm^{-3} within the channel region. I_D dependence on the

acceptor configuration (plotted by thin gray lines) becomes small as V_G increases under both drain voltages. Additionally, the difference between the jelly and the discrete impurity models decreases. These properties indicate that the present charge distribution model for the discrete impurities is screened by the carriers when the carrier concentration becomes large, and, thus, the configuration dependence becomes small. On the other hand, when V_G is small, I_D-V_G curves shows a significant configuration dependence. Therefore, the potential fluctuation induced by discrete impurity is mainly caused by the long-range Coulomb potential since the short-range potential depends on the acceptor concentration and is independent of the carrier concentration induced by V_G.

Table I summarizes V_{Th} under various calculation conditions, and statistical distributions of V_{Th} are found in Fig. 5 for V_D = 0.05 V and 0.8 V. Extracted standard deviations with SiO_2 layer are 13.4 mV and 14.4 mV under V_D = 0.05 V and 0.8 V, respectively. Those with HfO_2 are 10.2 mV and 11.2 mV, respectively. By using V_{Th} average and the standard deviation for each condition, the Gaussian distribution fits well the calculated result.

In the present Fin structure, the short-channel-effect (SCE) especially drain-induced-barrier-lowering (DIBL) is not negligible as the drain-voltage dependence of V_{Th} found in Table I and also Fig. 5. In the jelly doping cases, V_{Th} differences between those under V_D = 0.05 V and 0.8 V are 14.1 mV and 19.4 mV for SiO_2 and HfO_2, respectively. This difference between the SiO_2 and HfO_2 could be caused by a slight difference of gate capacitances. In the discrete impurity cases, V_{Th} under V_D = 0.8 V is shift to 15.7 mV and 22.2 mV for devices with SiO_2 and HfO_2, respectively, compared to the value under V_D = 0.05 V. The discrete model shows a larger shift than the jelly model, and the discrete impurity models with HfO_2 is weak to SCE in the present structure. This reason could be explained as follows: The electron concentration becomes large as approaching to the interface from the center of Si substrate when V_G is applied. On the other hand, the polarization correction dominates around the interface as presented in Figs. 2 (b) and (c). Therefore, it is expected that V_{Th} significantly depends on the concentration of acceptors and electrons at the interface. In the case with HfO_2, the correction term reduces the acceptor concentration and, thus, effective acceptor concentration, where $N_A = N_A^0 + \Delta N_A$, in the channel becomes smaller than the jelly concentration. In the device with SiO_2, the correction term increases the net-acceptor concentration around the interface and can suppress DIBL effect. As a result, V_{Th} shift with HfO_2 becomes larger than that with SiO_2.

The standard deviation reflects the strength of V_{Th} dependence on the acceptor configurations. When we consider the dependence of standard deviation on the drain voltage, the number of accepters in the region where the gate can dominantly control the potential in the channel. As a result, the number fluctuation in such a sensitive region also contributes to the statistical variability and, thus, results in an increase of the standard deviation in both cases. In the case with SiO_2, the acceptor concentration, $N_A = N_A^0 + \Delta N_A$, around the interface strongly depends on the position of acceptors since the correction term increases the acceptor concentration and is only significant around the interface as presented in Fig. 2 (b). On the other hand, the polarization in HfO_2 reduces the concentration fluctuation induced by the acceptor configurations as shown in Fig. 2 (c). It is because that the correction term reduces the net-acceptor concentration when an acceptor is close to the interface. As a result, the correction term weakens the acceptor configuration dependence. In summary, HfO_2 shows a smaller standard deviation than that with SiO_2.

IV. Conclusion

We have carried out 3D-DD simulation incorporated with discrete impurities modeled by Yukawa-like charge distributions. The discrete nature of impurities induces a polarization charge at the interface between the substrate and the oxide material depending on the difference of the dielectric constants. The present charge model produces the correct long-range Coulomb potential in the framework of DD device simulation. As a result, the screening of the long-range potential i.e., the potential fluctuation induced by the discrete impurity becomes dependent of the gate voltage and also carrier concentration in the channel region. The polarization correction term is able to distinguish the oxide material dependence of the potential fluctuation. It is inevitable for predictive device simulations to explicitly take into account the interface polarization induced by the discreteness of impurity.

TABLE I. Table of Threshold Voltages

Oxide	**SiO_2 (mV)**		**HfO_2 (mV)**	
Model	**Jelly**	**Discrete**	**Jelly**	**Discrete**
V_D = 0.05 V	140.0	140.4	132.5	115.6
V_D = 0.8 V	125.9	124.7	113.1	93.4

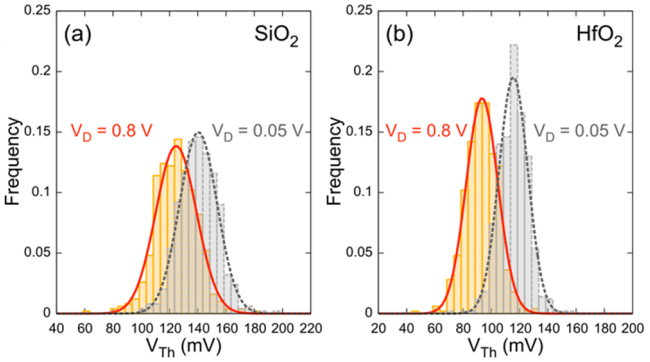

Fig. 5. Statistical distributions of threshold voltage for the devices with (a) SiO_2 and (b) HfO_2 gate oxides under V_D = 0.05 (orange) and 0.8 V (light-gray). Threshold voltage is defined when the drain current exceeds 14.3 nA/μm. The red solid and gray dotted curves are the Gaussian fits under V_D = 0.05 V and 0.8 V, respectively. The average of V_{Th} are summrized in Table I. For SiO_2 results, the standard deviations employed in Gaussian curves are 13.4 mV and 14.4 mV under V_D = 0.05 V and 0.8 V, respectively. Those values for HfO_2 are 10.2 mV and 11.2 mV under V_D = 0.05 V and 0.8 V, respectively.

Acknowledgment

This research was supported by MEXT as ‘‘Priority Issue on Post-K computer’’ (Creation of new functional Devices and high-performance Materials to Support next-generation Industries).

REFERENCES

[1] D. Hisamoto, W. C. Lee, J. Kedzierski, H. Takeuchi, and K. Asano, "FinFET-a self-aligned double-gate MOSFET scalable to 20 nm," IEEE Transactions on Electron Devices, vol. 47, no. 12, pp. 2320–2325, Dec. 2000, doi: 10.1109/16.887014.

[2] K. Nishinohara, N. Shigyo, and T. Wada, "Effects of Microscopic Fluctuations in Dopant Distributions on MOSFET Threshold Voltage," IEEE Transactions on Electron Devices, vol. 39, no. 3, pp. 634–639, Mar. 1992, doi: 10.1109/16.123489.

[3] H. S. Wong and Y. Taur, "Three-dimensional "Atomistic" Simu- lation of Discrete Random Dopant Distribution Effects in Sub-0.1 □/m MOSFET's," in IEDM Tech. Dig., 1993, pp. 705–708, doi: 10.1109/IEDM.1993.347215.

[4] Y. Li, C. H. Hwang, and T. Y. Li, "Random-Dopant-Induced Variability in Nano-CMOS Devices and Digital Circuits," IEEE Transactions on Electron Devices, vol. 56, no.8, pp. 1588–1597, Aug. 2009, doi: 10.1109/TED.2009.2022692.

[5] C. Shin, X. Sun, T. J. K. Liu, "Study of Random-Dopant-Fluctuation (RDF)Effects for the Trigate Bulk MOSFET," IEEE Transactions on Electron Devices, vol. 56, no. 7, pp. 1538–1542, Jul. 2009, doi: 10.1109/TED.2009.2020321.

[6] C. H. Hwang, Y. Li, and M. H. Han, "Statistical variability in FinFET de- vices with intrinsic parameter fluctuations," Microelectronics Reliability, vol. 50, pp. 635–638, Mar. 2010, doi: 10.1016/j.microrel.2010.01.041.

[7] L. Gerrer, A. R. Brown, C. Millar, R. Hussin, S. M. Amoroso, B. Chen, D. Reid, C. Alexander, D. Fried, M. Hargrove, K. Greiner, A. Asenov, "Accurate Simulation of Transistor-Level Variability for the Purposes of TCAD-Based Device-Technology Cooptimization," IEEE Transactions on Electron Devices, vol. 62, no. 6, pp. 1739–1745, Jun. 2015, doi: 10.1109/TED.2015.2402440.

[8] A. Asenov, G. Slavcheva, A. R. Brown, J. H. Davies, and S. Saini, "Increase in the Random Dopant Induced Threshold Fluctuations and Lowering in Sub-100 nm MOSFETs Due to Quantum Effects: A 3- D Density-Gradient Simulation Study," IEEE Transactions on Electron Devices, vol. 48, no. 4, pp. 722–729, Apr. 2001, doi:

[9] N. Sano, K. Matsuzawa, M. Mukai, and N. Nakayama, "On discrete random dopant modeling in drift-diffusion simulations: Physical meaning of 'atomistic' dopants," Microelectron. Rel., vol 42, no. 2, pp. 189–199, Feb. 2002, doi: 10.1016/S0026-2714(01)00138-X.

[10] N. Sano, K. Yoshida, C.-W. Yao, and H. Watanabe, "Physics of Discrete Impurities under the Framework of Device Simulations for Nanostructure Devices," Materials, vol. 11, pp. 2559, Dec. 2018, doi: 10.3390/ma11122559.